Available online at www.sciencedirect.com
ScienceDirect
Journal of Power Sources 165 (2007) 337–341
JOURNAL OF POWER SOURCES
www.elsevier.com/locate/jpowsour

Short communication

A compact and highly efficient natural gas fuel processor for 1-kW residential polymer electrolyte membrane fuel cells

Doohwan Lee, Hyun Chul Lee, Kang Hee Lee, Soonho Kim *

Energy and Materials Research Lab, Samsung Advanced Institute of Technology (SAIT), Mt. 14-1, Nongseo-dong, Giheung-gu, Yongin-si, Gyeonggi-do, 446-712, Republic of Korea

Received 16 August 2006; accepted 8 November 2006
Available online 22 January 2007

Abstract

A compact and highly efficient natural gas fuel processor for 1-kW residential polymer electrolyte membrane fuel cells (PEMFCs) has been developed at the Samsung Advanced Institute of Technology (SAIT). The fuel processor, referred to as SFP-2, consists of a natural gas reformer, a water–gas shift reactor, a heat-exchanger and a burner, in which the overall integrated volume including insulation is exceptionally small, namely, about 14 l. The SFP-2 produces hydrogen at 1000 l h^{-1} (STP) at full load with the carbon monoxide concentration in the process gas below 7000 ppmv (dry gas base). The maximum thermal efficiency is ~78% (lower heating value) at full load and even ~72% at 25% partial load. This fuel processor of small size with high thermal efficiency is one of the best such technologies for the above given H_2 throughputs. The time required for starting up the SFP-2 is within 20 min with the addition of external heating for the shift reactor. No additional medium, such as nitrogen, is required either for start-up or for shut down of the SFP-2, which is an advantage for application in residential PEMFC co-generations systems.

Keywords: Fuel processor; Polymer electrolyte membrane fuel cell; Hydrogen; Residential system; Natural gas

1. Introduction

Fuel cells are highly efficient electric power generation systems. In particular, polymer electrolyte membrane fuel cells (PEMFCs) combined with cogeneration systems are of great interest for residential applications [1,2]. This application offers two benefits: (i) on site and real time generation of electricity with a high efficiency; (ii) utilization of the heat produced during operation of fuel cells for hot water generation and house heating. In providing hydrogen for this application, on site production via conversion of natural gas appears to be currently the most practical. This is because, setting aside the difficulties in the transportation and storage of hydrogen, natural gas is cost effective, abundant in nature and easily deliverable to individual houses via available and extensive pipeline infrastructures. Many aspects of fuel processors should be considered for this application, e.g., time and energy consumption for start-up, thermal efficiency, transient response during changes of hydrogen throughput, concentration of carbon monoxide in the process gas stream, size and life time. These aspects depend significantly on the thermodynamics and kinetics of the catalytic reactions involved, as well as on construction and integration of the reactor units. There have been a number of studies of fuel processing methods [3,4] and reactor technologies [5–12] for the production of H_2 from various hydrocarbon fuels.

In this work, we present a compact and highly efficient natural gas fuel processor, referred to as SFP-2, that has been developed at Samsung Advanced Institute of Technology (SAIT). The SFP-2 consists of a reformer, a water–gas shift reactor, a heat-exchanger and a burner, in which the overall volume including insulations is only around 14 l. Details of the construction of each reactor unit and their integration in SFP-2 are presented. The performance is analyzed and discussed in terms of the thermodynamics and kinetics of the methane steam reforming (MSR) and water–gas shift (WGS) reactions, as well as the heat utilization in the integrated fuel processor.

2. Thermodynamics and kinetics

Methane steam reforming Eq. (1) was chosen in this work, because it offers a high H_2 concentration in the

* Corresponding author. Tel.: +82 31 280 8155; fax: +82 31 280 9359.
E-mail address: kimsoonho@samsung.com (S. Kim).

0378-7753/$ – see front matter © 2006 Elsevier B.V. All rights reserved.
doi:10.1016/j.jpowsour.2006.11.073

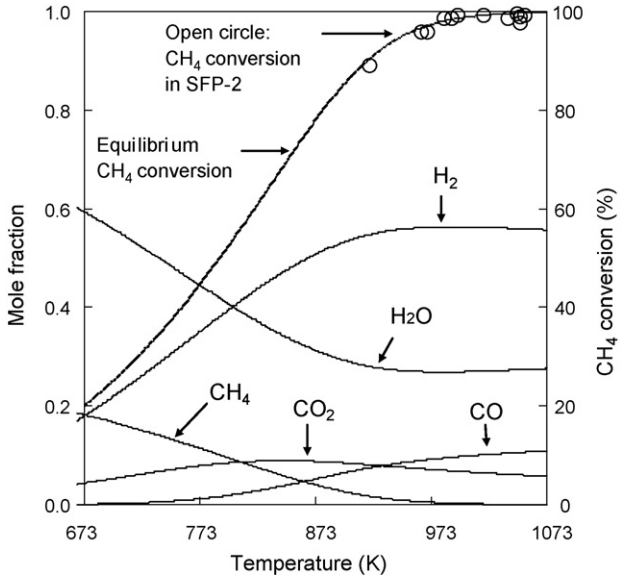

Fig. 1. CH_4 conversion and product concentration as a function of temperature. Lines: Equilibrium CH_4 concentration and product concentration at S/C ratio of 3. Open circles: Experimental CH_4 conversion obtained in the reformer.

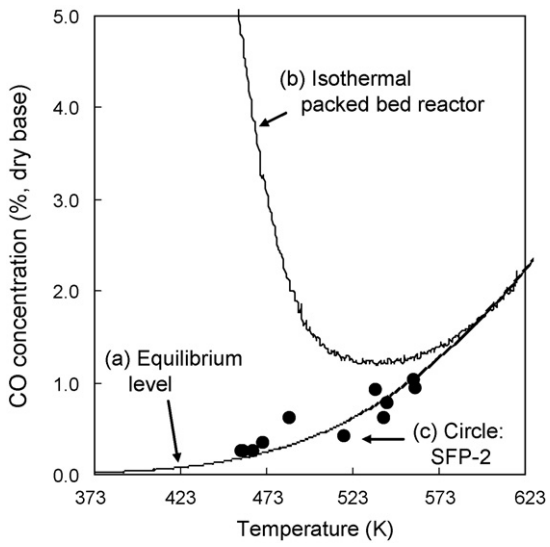

Fig. 2. Equilibrium and experimental CO concentration as a function of temperature. Composition of reactant stream = 7% CO, 26% H_2O, 7% CO_2 and 60% H_2O. (a) Equilibrium CO concentration; (b) CO concentration obtained in an isothermal packed-bed reactor using a commercial copper-based catalyst at GHSV of 6000 h^{-1}; (c) CO concentration in the process gas obtained in the WGS reactor.

reaction products.

$$CH_4 + H_2O \rightleftarrows CO + 3H_2, \quad \Delta H_{298} = 49\,\text{kcal mol}^{-1} \qquad (1)$$

The reforming reaction is accompanied by the subsequent WGS reaction Eq. (2), in which the CO formed via the steam reforming reacts with water to produce additional H_2 and CO_2.

$$CO + H_2 \rightleftarrows CO_2 + H_2, \quad \Delta H_{298} = -10\,\text{kcal mol}^{-1} \qquad (2)$$

The stoichiometry for the complete CH_4 and CO conversions via the above reactions requires a steam-to-carbon molar ratio (S/C) of two. In practical applications, however, a S/C ratio of greater than two is preferable in order to suppress deactivation of reforming catalysts. This is because a local deficiency of water vapour due to uneven distribution of the reactants results in carbon formation which, in turn, leads to deactivation of the catalysts. The MSR is highly endothermic and therefore requires elevated temperatures for high CH_4 conversion. By contrast, the WGS reaction is exothermic and thus low temperatures are necessary for high CO conversion. Fig. 1 shows the equilibrium CH_4 conversion (S/C = 3) and product concentration as a function of temperature. The equilibrium CH_4 conversion increases with an increase in temperature and reaches over 95% at above ~950 K. The CO formed via the MSR is partially converted to CO_2 via the WGS reaction within the extent of the equilibrium level. For comparison, experimental CH_4 conversions are also presented as a function of the exterior surface temperature of the reformer as measured near the reformate exit. The results show that CH_4 conversions reached to the equilibrium levels at the measured reformer temperatures. It is often discussed that highly endothermic nature of the MSR can result in a heat-transfer limitation. In this study, the good agreement between the equilibrated experimental CH_4 conversions and measured temperatures obtained in the reformer indicate that heat transfer was not limiting. This was mostly due to the high surface-area to volume ratio of the catalyst bed in the reformer that maximized the heat-transfer area.

In contrast to the MSR, temperature causes an antagonistic effect on the rate and equilibrium CO conversion in the WGS reaction due to the exothermic character of the reaction. Fig. 2 shows the The equilibrium CO concentration calculated as a function of temperature for an approximate reformate concentration (7.4% CO, 26.0% H_2O, 7.4% CO_2, 60.0% H_2). The experimental CO concentration obtained in an isothermal, packed-bed reactor using a copper-based catalyst is also displayed (GHSV=6000 h^{-1}). As displayed, the CO concentration in the product stream experienced a minimum value at ~530 K due to a trade-off between the limited equilibrium CO conversions at high temperatures and the low catalytic CO conversion rates at low temperatures.

The reversible nature of the MSR and WGS reactions and the effect of temperature on equilibrium conversion and reaction rate give a guideline for the construction of each reactor which is practically operated at non-isothermal conditions. Fig. 3 illustrates the temperature profiles in the reformer and WGS reactor of the SFP-2, as well as the development of the respective CH_4 conversion and CO concentration. In the reformer, an increase in temperature along the direction of the reactant flow path was achieved by giving a counter-current configuration between the reactants and the exhaust gas of the burner. This maximized heat recovery from the exhaust gas and developed a temperature profile that was thermodynamically preferable for high CH_4 conversion. In the WGS reactor, a decrease in temperature along the direction of the reactant flow path was established in order to maximize the catalytic CO conversion rate and alleviate the equilibrium limitation. As shown in Fig. 2 the experimental CO concentration in the process gas obtained in the WGS reactor reached the equilibrium levels at the low

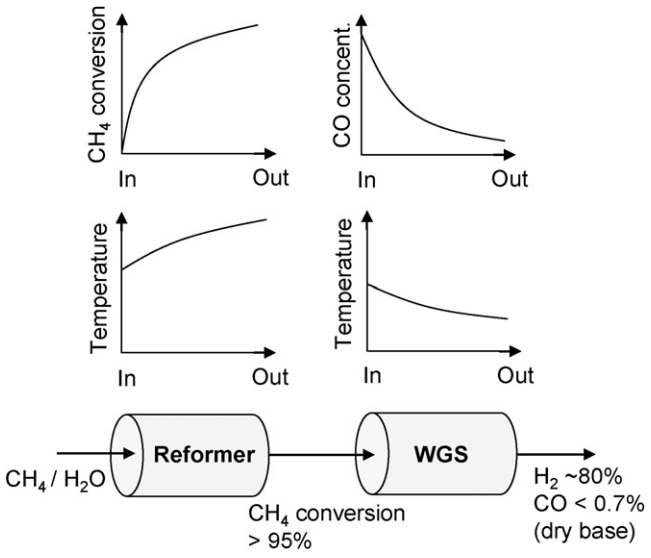

Fig. 3. Illustration of temperature profile in the reformer and WGS reactor and corresponding CH_4 conversion and CO concentration.

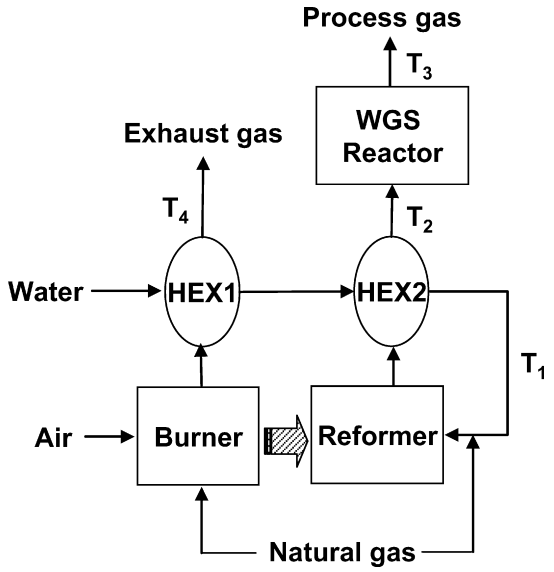

Fig. 5. Schematic of the fuel processing procedure in the SFP-2. HEXs: heat-exchangers.The CH_4, H_2O and air feeds were at ambient temperatures.

temperatures, which was not achievable under an isothermal condition.

From the above thermodynamic and kinetic investigation on the MRS and WGS reactions, it is clear that a positive temperature gradient in the catalyst bed of the MSR reactor with respect to the reactant flow path is required, while in the WGS reactor a negative temperature gradient is necessary. All of these aspects assisted the integration of the fuel processor.

3. Integration of fuel processor

A commercial Ru-based catalyst (spherical shape, 3 × 3 mm) was used for the MSR reaction and a commercial Cu-based catalyst (cylindrical shape, 3 × 3 mm) was used for the WGS reaction. A photograph and schematic of the integrated SFP-2 without external insulation is given in Fig. 4. The volume of the SFP-2 was approximately 6.5 l without external insulation and 1 4 l. The SFP-2 consisted of a reformer, a WGS reactor, a heat-exchange assembly, and a burner. The reformer was concentrically placed inside the annular-shaped WGS reactor with insulation between these two reactors. The burner was located on the bottom of the reformer in order to supply heat directly to the reformer. The heat-exchanger assembly consisted of two basic units (HEX1 and HEX2; Fig. 5) and was placed on top of the reactor assembly. Finally, the external surface of this integrated SFP-2 was insulated. A schematic of the fuel-processing procedure implemented in the SFP-2 is shown in Fig. 5. The reactant H_2O was partially evaporated at HEX1 by heat-exchanging with the burner exhaust gas and completely evaporated at HEX2 by heat-exchanging with the reformate gas from the reformer. It was then mixed with the CH_4 feed at a required S/C ratio and introduced into the reformer. The reformate products were subsequently introduced into the WGS reactor for additional CO conversion. This finally produced the process gas that contained a high concentration of H_2 (near 80 vol.%, dry base) with low concentration of CO (below 7000 ppmv, dry base).

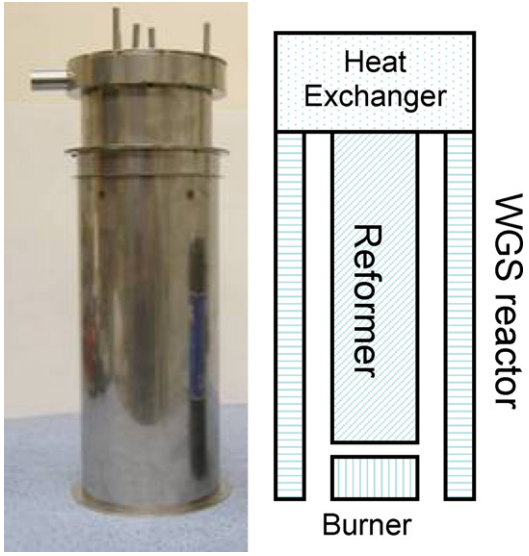

Fig. 4. Photograph and schematic of integrated SFP-2.

4. Experimental and analysis

The performance of SFP-2 was tested in a laboratory-built test station equipped with flow control units, temperature and pressure recorders and gas analyzers. The reactants were CH_4 (zero grade) and de-ionized water. The flow rate of CH_4 was controlled by a mass-flow controller (Brooks, 5850E) and that of water was regulated by a HPLC pump (LabAlliance, Series II). The compositions of the process and exhaust gases were analyzed by various analytical techniques, namely: gas chromatography for quantitative gas analysis; non-dispersive infrared (NDIR) for real-time carbon monoxide; carbon dioxide, methane and hydrogen measurements. The temperature distribution in the fuel processor and at the process stream was recorded simul-

taneously. Basically, four operation parameters were derived in order to evaluate and analyze the performance of the SFP-2: (i) CH_4 feed rate to the reformer; (ii) steam-to-carbon molar ratio in the feed to the reformer (S/C ratio); (iii) reformer-to-burner CH_4 feed ratio (R/B $= (n_{CH_4,reformer}/n_{CH_4,burner})$); (iv) ratio of actual air feed rate to the stoichiometrically required air feed rate for a complete combustion of the CH_4 feed in the burner ($\lambda = (n_{actural\ air\ feed\ rate}/n_{stoichiometrical\ air\ feed\ rate})$). The efficiency ($\eta$) of the SFP-2 was calculated using the following equation:

$$\text{Efficiency}\,(\eta, \text{LHV}) = \frac{n_{H_2}}{n_{CH_4,reformer} + n_{CH_4,burner}} \times \frac{\Delta H_{H_2}}{\Delta H_{CH_4}} \quad (3)$$

where n_{H_2} is the H_2 throughput (mol h^{-1}), $n_{CH_4,reformer}$ is the CH_4 feed rate (mol h^{-1}) to the reformer, $n_{CH_4,burner}$ is the CH_4 feed rate (mol h^{-1}) to the burner, ΔH_{H_2} is the lower heating value (LHV) of H_2, and ΔH_{CH_4} is the lower heating value of CH_4, respectively.

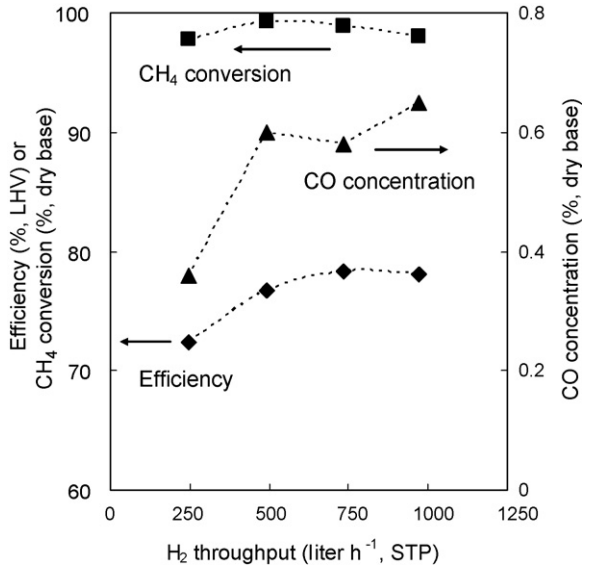

Fig. 6. Maximum efficiency (LHV) and corresponding CH_4 conversion and CO concentration at various H_2 throughputs in SFP-2.

5. Results and discussion

The CH_4 conversion depended significantly on temperature of the reformer, which was governed mainly by the balance between the heat supplied from the burner and that consumed by the reformer. An increase in the CH_4 conversion caused by an increase in the burner power (i.e., decrease in the R/B ratio) generally led to an increase in the efficiency due to an enhancement in H_2 throughput, but this dependency was reduced at CH_4 conversions above ~95%. This was reasonable because an excess of heat supplied to the reformer did not lead to a significant enhancement in H_2 throughput as the CH_4 conversion approached 100%. The efficiency obtained at various steam-to-carbon ratios (S/C = 3–5) indicated that an increase in the S/C ratio led to a decrease in the efficiency. At high S/C ratios enhanced CH_4 and CO conversion was expected from the reaction equilibrium and kinetics, but the energy required to evaporate and heat up the reactant water to the reaction temperatures was significantly high, and resulted in a net decrease in the efficiency.

The CO concentration in the process gas stream was sensitive to the temperature of the WGS reactor. As discussed, the adverse effect of temperature on the thermodynamic equilibrium and the reaction kinetics requires the WGS reaction to be operated in an optimum temperature range for the maximum CO conversion. Detailed calculation of the mass and energy balance in the SFP-2 were conducted, and the results were used in the integration of the reactor and heat-exchanger units in order to obtain an adequate temperature distribution in the WGS reactor at various H_2 throughput conditions. Consequently, CO concentrations in the process gas below ~7000 ppmv (dry gas base) were obtained at the maximum efficiencies for the entire H_2 throughputs. The results are shown in Fig. 6. It should be noticed that the CO concentration could be reduced to below a few thousand ppmv levels with a slight expense in the efficiency by increasing the S/C ratio or the R/B ratio.

The efficiency decreased as the H_2 throughput decreased, as commonly seen in any type of fuel processor. To discuss this, it would be reasonable to calculate the maximum theoretical efficiency that can be achieved without any energy loss. For a complete CH_4 conversion ($CH_4 + 2H_2O \rightarrow CO_2 + 4H_2$), the energy carried in a CH_4 reactant feed of 250 l h^{-1} is 2462 kcal h^{-1} (LHV), and that in the H_2 product feed of 1000 l h^{-1} is 2140 kcal h^{-1}. The energy required for complete CH_4 conversion at 973 K at the given flow rate is 508 kcal h^{-1}. If account is taken of the energy required to raise the temperature of the CH_4 and H_2O reactants to 973 K and it is assumed that the temperature of the process gas is 393 K, the maximum theoretically achievable efficiency is approximately 82%. Some energy loss on the surface of fuel processor and through the burner exhaust gas stream is inevitable, and clearly this will result in a decrease in the efficiency.

As discussed previously, the thermodynamic equilibrium and kinetics determine the optimum temperature range for the MSR and the WGS reactions. This temperature range does not change significantly with the reactant feed rates and therefore the energy loss from the surface of a fuel processor will be similar at various H_2 throughput conditions. As a consequence, the fraction of the energy loss compared with the energy in the produced H_2 steam becomes larger as the H_2 throughput becomes smaller. This results in a decrease in the efficiency. Table 1 shows the maximum efficiencies obtained at various H_2 throughputs in the SFP-2 and the corresponding average temperatures in the reformer and WGS reactors as well as in the process streams. The data show that the average temperatures in the reformer and WGS reactor did not vary significantly at these H_2 throughput conditions. In fact, energy balance calculations using the temperature of the process stream and product compositions indicated that only a small energy loss occured in the SFP-2. The resulting high efficiencies obtained in the SFP-2 are among the best for natural gas fuel processors at the similar H_2 throughput ratings. It

Table 1
Summary of performance of SFP-2

Load (%)	H_2 throughput ($l h^{-1}$, STP)	Efficiency (%, LHV)	Process gas composition (%, dry base)				Average temperature (K)		Temperature at processing stream (K, Fig. 5)			
			H_2	CO_2	CH_4	CO	Reformer	WGS	T_1	T_2	T_3	T_4
25	240	72.4	79.60	19.63	0.41	0.36	850	480	373	339	395	387
50	490	76.7	79.75	19.49	0.16	0.60	930	510	373	347	416	377
75	740	78.3	79.70	19.49	0.23	0.58	890	520	373	362	427	371
100	970	78.1	79.53	19.40	0.42	0.65	890	520	373	374	435	378

is clear from the results that the markedly high efficiencies were mainly due to good thermal integration as well as the small size of the SFP-2, which reduce the energy loss from the surface.

Finally, some remaining issues that need to be addressed are the CO concentration in the process gas steam, anode-off gas utilization, time and energy required for start-up and additional procedures for operation of the fuel processor. In particular, it is known that CO irreversibly poisons the Pt-group catalysts of the anode of PEMFCs. The preferential oxidation of CO (PROX; $CO + 1/2O_2 \rightarrow CO_2$) is effective for removal of residual CO to below tens of ppm levels, which is required for the applications in PEMFCs. The performance of PROX, however, mainly depends on the activity and selectivity of the catalysts. Therefore, instead of presenting the performance of the PROX reactor, details of the activity and selectivity of the catalysts developed at SAIT will be reported in a separate paper. The anode off-gas utilization and time and energy requirement in the start-up of SFP-2 are not discussed in this work, because it is more reasonable to consider them in conjunction with integration and operation of the overall fuel-cell system. Several experimental studies, however, showed that the SFP-2 reached a practical working condition (CH_4 conversion >95%, CO concentration <7000 ppmv) within 20 min with an additional external heating on the shift reactor. No additional medium was necessary in the operation of the SFP-2. This features provide more convenient and practical applications for residential PEMFC co-generations systems.

6. Conclusions

A compact and highly efficient natural gas fuel processor developed at Samsung Advanced Institute of Technology (SAIT), referred to as the SFP-2, was presented. The volume of the SFP-2 was small, namely, ~14 l including insulation. The efficiency was above 72% at the entire turn-down ratio. The maximum efficiency was 78% at the full operation load (H_2 throughput = ~1000 $l h^{-1}$) and the CO concentration in the process gas stream was below 7000 ppmv. Analysis on the performance of the SFP-2 indicated that excellent construction and integration of the reactor units gave rise to high CH_4 and CO conversions, as well as good heat recovery. These attributes resulted in markedly high efficiencies for the entire turn-down ratio.

References

[1] H.I. Onovwiona, V.I. Ugursal, Renew. Sust. Energy Rev. 10 (2006) 389–431.
[2] H. Aki, S. Yamamoto, J. Kondoh, T. Maeda, H. Yamaguchi, A. Murata, I. Ishii, Int. J. Hydrogen Energy 31 (2006) 967–968.
[3] C. Song, Catal. Today 77 (2002) 17–49.
[4] T.A. Semelsberger, R.L. Borup, Int. J. Hydrogen Energy 30 (2005) 425–435.
[5] D.J. Moon, K. Sreekumar, S.D. Lee, B.G. Lee, H.S. Kim, Appl. Catal. A: Gen. 215 (2001) 1–9.
[6] D.G. Löffler, K. Taylor, D. Mason, J. Power Sources 117 (2003) 84–91.
[7] J.R. Lattner, M.P. Harold, Int. J. Hydrogen Energy 29 (2004) 393–417.
[8] M.P. Harold, B. Nair, G. Kolios, Chem. Eng. Sci. 58 (2003) 2551–2571.
[9] S.H.D. Lee, D.V. Applegate, S. Ahmed, S.G. Calderone, T.L. Harvey, Int. J. Hydrogen Energy 30 (2005) 829–842.
[10] M. Echigo, N. Shinke, S. Takami, T. Tabata, J. Power Sources 132 (2004) 29–35.
[11] J. Han, I.-S. Kim, K.-S. Choi, Int. J. Hydrogen Energy 27 (2002) 1043–1047.
[12] J. Mathiak, A. Heinzel, J. Roes, T. Kalk, H. Kraus, H. Brandt, J. Power Sources 131 (2004) 112–119.